

# NON-PARAMETRIC SPECTRUM CARTOGRAPHY USING ADAPTIVE RADIAL BASIS FUNCTIONS

*Mohamed Hamid and Baltasar Beferull-Lozano*

WISENET Lab., Dept. of ICT, University of Agder, Grimstad, Norway

## ABSTRACT

This paper presents a framework for spectrum cartography based on the use of adaptive Gaussian radial basis functions (RBF) centered around a specific number of centroid locations, which are determined, jointly with the other RBF parameters, by the available measurement values at given sensor locations in a specific geographical area. The spectrum map is constructed non-parametrically as no prior knowledge about the transmitters is assumed. The received signal power at each location (over a given bandwidth and time period) is estimated as a weighted contribution from different RBF, in such a way that the both RBF parameters and the weights are jointly optimized using an alternating minimization method with a least squares loss function and a quadratic regularization term. Our method is evaluated through simulations, showing a performance (in terms of normalized MSE) that is comparable to semi-parametric methods, and even superior as the number of sensors or RBF increases.

**Index Terms**— Spectrum Cartography, Radial Basis Functions, Alternating Minimization.

## 1. INTRODUCTION

Spectrum cartography is the process of building spatial, frequency and time dependent radio environment maps (REMs) [1]. The REMs can be constructed for different radio parameters such as received signal power, channel gains and interference. For the sake of simplicity, throughout the rest of this paper, REMs and spectrum cartography will be used interchangeably with the assumption that they refer to received signal power maps. Building REMs is convenient for many applications including network planning, frequency reuse, coverage prediction, interference management, opportunistic spectrum access and cognitive radios [2–5]. A fundamental task for REM construction is to collect geo-localized measurements and thereafter perform spatial interpolation to have a full map [6].

There have been several proposed techniques for spatial interpolation with an aim of obtaining REMs. Kriging interpolation is one of these techniques used in [6, 7] where the

received signal power at each point is estimated as a weighted sum of the available measurements. In [8], Kriging interpolation is extended to track the transmitter time-varying activity using Kalman filtering. Dictionary learning is used in [9] for spectrum cartography where the adjacency matrix is used to exploit the correlation among the measurements coming from neighboring nodes. Sparsity in frequency domain is used for spectrum cartography in [10]. In [11], a spectrum cartography framework has been developed using a basis expansion model based on solving a variational optimization problem involving thin-plate smoothing splines. In [12], spectrum cartography is formulated as a matrix completion problem to estimate REMs with the aid of existing cellular infrastructure. The contributions in [13–15] use reproducing kernel Hilbert space (RKHS) and semi parametric models for spectrum cartography. While having diverse current solutions for spectrum cartography with these techniques, they are however having at least one of the following three limitations. At first, they are either fully or in part parametric techniques where some information regarding the transmitters' parameters and locations are needed. Secondly, a spatially high density measurements are needed which is very costly in terms of energy and communication bandwidth. Finally, basis functions or kernels' parameters are not chosen adaptively depending on the measurements.

This paper is motivated to overcome these aforementioned limitations by developing a non-parametric spectrum cartography algorithm where the parameters of the basis functions are updated based on a lower density of measurements as compared to previous work. By non-parametric here, it is meant that the model has no parameters that depend on transmitters' locations or power spectral densities (PSDs). For achieving this goal, a linear combination of adaptive Gaussian radial basis functions (RBF) are suggested in this paper with no prior knowledge about the transmitters. RBF are used because of their ability for fitting high non-linear functions [16]. Moreover, most of the propagation models assume isotropic antennae since the average received power is modeled as a function of only the Euclidean distance from the transmitter with no consideration of the angles. In this regard, RBF are used as they require only Euclidean distance dependent systems [17]. In this paper, the RBF are centered around representative centroids that represent strategic informative loca-

This work was supported by the FRIPRO TOPPFORSK grant 250910/F20 from the Research Council of Norway.

tions instead of directly using the sensors locations to center the RBF. Our numerical results show that, even-though our approach in non-parametric with respect to the transmitters, the proposed algorithm compensate for the lack of transmitters' information by adapting the RBF centers locations and parameters.

The rest of this paper is organized as follows. Section 2 illustrates the system model in terms of problem formulation and the theoretical aspects of the RBF-based cartography. Section 3 presents the main contribution of the paper which is adaptive RBF with representative centroids based cartography. Simulations and findings interpretations are shown in Section 4. Finally, Section 5 concludes the paper.

## 2. SYSTEM MODEL

### 2.1. Problem Statement

Assume  $M$  radio transmitters operating at frequency  $f$ , and located within a geographical area,  $\mathcal{R} \subset \mathbb{R}^2$ . Suppose that these radios use time-dependent uncorrelated transmitted PSDs, denoted as  $\xi_m(f, t)$  for each  $m^{\text{th}}$  transmitter at time  $t$ . Consequently, the time-dependent received signal power at location  $\mathbf{x}$ , which we denote as  $h(\mathbf{x}, f, t)$ , is given by:

$$h(\mathbf{x}) = \sum_{m=1}^M \int_T \int_{BW} |G(\mathbf{x}, \mathbf{x}_m, f, t)|^2 \xi_m(f, t) df dt \quad (1)$$

with  $BW$  being the bandwidth we are aggregating energy over.  $T$  is a certain considered time period during which there is an aggregation of maps.  $G(\mathbf{x}, \mathbf{x}_m, f, t)$  is a filter characterizing the channel frequency response between the intended location,  $\mathbf{x}$ , and the  $m^{\text{th}}$  transmitter location,  $\mathbf{x}_m$ .

In many applications, such as spectrum sensing in cognitive radios or when the transmitter is a license exempt user as in the ISM band, none of the transmitters' PSDs, locations and the channel frequency response are known to the receivers. Therefore, the complete spectrum cartography is estimated using a finite set of measurements,  $\mathcal{Y} = \{y_1, y_2, \dots, y_n\}$ ,  $1 \leq n \leq N$  gathered by a set of receivers with a locations' set  $\mathcal{X} = \{\mathbf{x}_1, \mathbf{x}_2, \dots, \mathbf{x}_n\}$ . The estimated cartography will be denoted from here on as  $\hat{h}(\mathbf{x})$  where  $\hat{h}(\mathbf{x}) : \mathcal{X} \rightarrow \mathcal{Y}$ , while the actual cartography is denoted as  $h(\mathbf{x})$ . It is assumed that there exist a fusion center that receives  $\mathcal{X}$  and  $\mathcal{Y}$  from the measurements' nodes and estimates the cartography.<sup>1</sup>

### 2.2. RBF-Based Cartography

This part of the paper reviews the theory of using RBF spectrum cartography learning. The RBF learning model is based on assuming that each point on the learning sets,  $(\mathbf{x}_n, y_n)$ ,

<sup>1</sup>For future work, we are considering a fully distributed approach through local communications among neighboring sensor nodes.

affects the target function on any location  $\mathbf{x}$  as a function of the Euclidian distance between  $\mathbf{x}$  and  $\mathbf{x}_n$  [17]. With respect to spectrum cartography and the standard form of RBF, the assumed learning model is formulated as:

$$h(\mathbf{x}) = w_0 + \sum_{i=1}^{\infty} w_i \exp(-\gamma_i \|\mathbf{x} - \mathbf{x}_i\|^2) \quad (2)$$

where  $w_0$  is a constant offset that is useful when  $h(\mathbf{x})$  has a large  $\mathbf{x}$ -independent component [16]. In our case, this independent component is the background noise, in particular when no transmission is active and only noise is received.  $w_1, \dots, w_{\infty}$ , are weighting parameters for the influence of the different RBF,  $\gamma_i$  is a Gaussian decaying parameter for the  $i^{\text{th}}$  RBF.

When considering only the available  $N$  measurements, then we have:

$$w_0 + \sum_{i=1}^N w_i \exp(-\gamma_n \|\mathbf{x}_n - \mathbf{x}_i\|^2) = y_n \quad (3)$$

which can be expressed in matrix form as:

$$\Phi \mathbf{w} = \mathbf{y} \quad (4)$$

where  $\Phi = [\mathbf{1}_N \mid \tilde{\Phi}]$ ,  $\mathbf{1}_l$  is the all-one column vector of size  $l$  and  $\tilde{\Phi} \in \mathbb{R}^{N \times N}$  with each element being  $\tilde{\Phi}_{nk} = \exp(-\gamma_k \|\mathbf{x}_n - \mathbf{x}_k\|^2)$

If  $w_0$  is known, then solving (4) for  $\mathbf{w}$  as  $\mathbf{w} = \Phi^{-1} \mathbf{y}$  implies finding  $N$  parameters from  $N$  observations which yields an *exact interpolation* on the learning sets  $\mathcal{X}$  and  $\mathcal{Y}$ . However, exact interpolation is not only computationally expensive for large data sets, but may also create *overfitting* problems as the measurements noise is not accounted for [17]. Numerical stability is also a problem if two sensors are very close to each other.

## 3. ADAPTIVE RBF WITH REPRESENTATIVE CENTRIODS USING ALTERNATING MINIMIZATION ALGORITHM

Consider  $K$  centroids which are denoted as  $\mu_1, \dots, \mu_K$ , then the cartography learning model becomes:

$$\hat{h}(\mathbf{x}) = w_0 + \sum_{k=1}^K w_k \exp(-\gamma_k \|\mathbf{x} - \mu_k\|^2) \quad (5)$$

Given  $N$  measurements, the updated model involving  $K$  centroids in matrix form is

$$\Theta \mathbf{w} = \mathbf{y} \quad (6)$$

where  $\Theta = [\mathbf{1}_K \mid \tilde{\Theta}]$ ,  $\tilde{\Theta} \in \mathbb{R}^{N \times K}$  composed as  $\tilde{\Theta}_{nk} = \exp(-\gamma_k \|\mathbf{x}_n - \mu_k\|^2)$ ,  $1 \leq n \leq N, 1 \leq k \leq K$ .

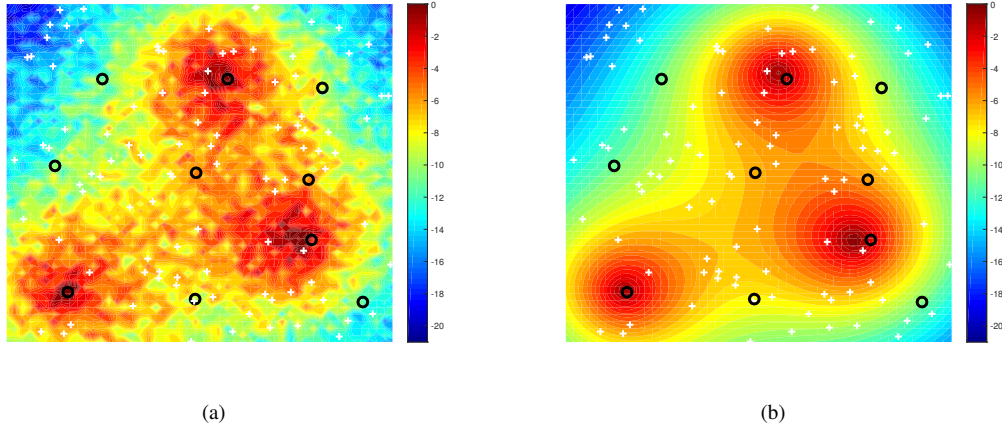


**Fig. 1.** (a) Actual cartography. (b) Estimated cartography using 100 measurements and 10 centroids. Sensors locations are shown as white crosses while optimized centroids locations are represented by black circles

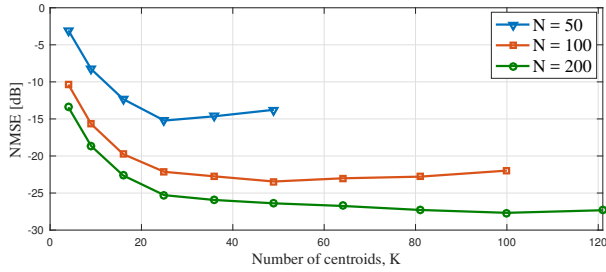


**Fig. 2.** Estimated cartography NMSE for different values of number of measurements,  $N$  and centroids,  $K$

To estimate the cartography on  $\mathcal{R}$ , we need to initialize and optimize the model parameters including: a) the centroids,  $\mu_1, \dots, \mu_K$ , b) the weights vector  $\mathbf{w}$  and c) the Gaussian decaying parameters  $\gamma_1, \dots, \gamma_K$ .

In order to optimize jointly the weights vector  $\mathbf{w}$ , centroids locations,  $\mu_1, \dots, \mu_K$ , and the Gaussian decaying parameters  $\gamma_1, \dots, \gamma_K$ , a Least Squares (LS) solution is considered as follows:

$$\min_{\mathbf{w}, \gamma_1, \dots, \gamma_K, \mu_1, \dots, \mu_K} \sum_{n=1}^N \left( y_n - \hat{h}(\mathbf{x}_n) \right)^2 + \lambda \|\mathbf{w}\|^2 \quad (7)$$

where  $\hat{h}(\mathbf{x}_n)$  is obtained by (5),  $\lambda$  is a positive constant that trades off between the squared norm of  $\mathbf{w}$  and a loss function expressing the goodness of fit.  $\lambda = 0.5$  is used in this paper. Besides reducing the variance of the estimation error, norm-2 regularization also guarantees a solution to (7) even if  $\Theta\Theta^T$  is a singular matrix (i.e. see (8) below) [18]. In the case of cartography this would happen in the case of either strong fading and shadowing or when no transmission takes place and only background noise is received. Moreover, In the case of some of the resulting centroids are very close to each other,

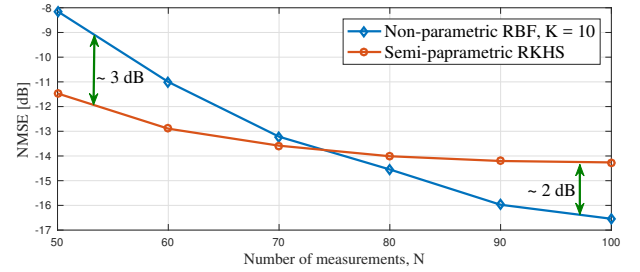


**Fig. 3.** Performance comparison between the proposed non-parametric RBF technique and the semi-parametric RKHS based technique proposed in [14]

$\Theta\Theta^T$  is a singular matrix also.

To solve the optimization problem (7) for  $\mathbf{w}$ ,  $\mu_1, \dots, \mu_K$ , and  $\gamma_1, \dots, \gamma_K$ , we propose to use a gradient decent (GD) based alternating minimization method. Notice however that if  $\gamma_1, \dots, \gamma_K$  and  $\mu_1, \dots, \mu_K$  are fixed, then a closed form LS solution for (7) with respect to  $\mathbf{w}$  can be obtained by

$$\mathbf{w} = (\Theta^T \Theta + \lambda \mathbf{I}_K)^{-1} \Theta^T \mathbf{y} \quad (8)$$

where  $\mathbf{I}_K$  denotes a  $K \times K$  identity matrix. It should be noted that even in cases where the inverse in (8) is numerically unstable or computationally expensive, one could still use GD approach to find  $\mathbf{w}$ , without taking any inverse. To solve (8),  $\Theta$  is initialized by assigning a constant value for the decaying parameters,  $\gamma_1, \dots, \gamma_K$ . For initializing the centroids in a meaningful manner,  $K$ -mean clustering [19] is used by splitting the input set into  $K$  clusters,  $\mathcal{S}_1, \dots, \mathcal{S}_K$  and then, the centroids of these clusters are found considering the well-known objective

$$\min_{\mathcal{S}_k, \mu_k} \sum_{k=1}^K \sum_{\mathbf{x}_n \in \mathcal{S}_k} \|\mathbf{x}_n - \mu_k\|^2 \quad (9)$$

Given that this is a non-convex set, we can use the iterative Lloyd's algorithm to find a solution for (9) which involves two basic iterations [20]

$$\mu_k \leftarrow \frac{1}{|\mathcal{S}_k|} \sum_{\mathbf{x}_n \in \mathcal{S}_k} \mathbf{x}_n \quad (10a)$$

$$\mathcal{S}_k \leftarrow \{\mathbf{x}_n : \|\mathbf{x}_n - \mu_k\| < \|\mathbf{x}_n - \mu_l\|, \forall l \neq k\} \quad (10b)$$

After their initialization, the GD updates at time slot  $i$  for the decaying parameters  $\gamma_1, \dots, \gamma_K$  and the centroids  $\mu_1, \dots, \mu_K$  assuming a step-size  $\alpha$  are given by :

$$\begin{aligned} \gamma_k^i &= \gamma_k^{(i-1)} - \alpha \sum_{n=1}^N \left( (y_n - \hat{h}(\mathbf{x}_n)) \cdot \|\mathbf{x}_n - \mu_k\|^2 \cdot \right. \\ &\quad \left. (w_k \exp(-\gamma_k \|\mathbf{x}_n - \mu_k\|^2)) \right) \end{aligned} \quad (11)$$

$$\begin{aligned} \mu_k^i &= \mu_k^{(i-1)} + 2\alpha\gamma_k \sum_{n=1}^N \left( (y_n - \hat{h}(\mathbf{x}_n)) \cdot (\mathbf{x}_n - \mu_k) \cdot \right. \\ &\quad \left. (w_k \exp(-\gamma_k \|\mathbf{x}_n - \mu_k\|^2)) \right) \end{aligned} \quad (12)$$

To summarize, an iterative alternating minimization method is adopted in the following steps

1. Initialize the centroids using (10a) and (10b) iteratively.
2. Fix  $\gamma_1, \dots, \gamma_K, \mu_1, \dots, \mu_K$  and solve for  $\mathbf{w}$  using (8).
3. Fix  $\mathbf{w}, \mu_1, \dots, \mu_K$  and solve for  $\gamma_1, \dots, \gamma_K$ , using GD as in (11).
4. Fix  $\mathbf{w}, \gamma_1, \dots, \gamma_K$  and solve for  $\mu_1, \dots, \mu_K$ , using GD as in (12).
5. Iterate 2-4 till all of the parameters converge.

## 4. SIMULATIONS AND NUMERICAL RESULTS

### 4.1. Simulations Setup

A  $50m \times 50m$  indoor area contains three active transmitters arbitrary located and  $N$  sensing nodes uniformly randomly spread over the area is considered for simulations assuming a pathloss model developed in [21] with its used parameters as in [21, 22]. Both the area and the propagation model are chosen arbitrarily as representatives to verify the functionality of the proposed cartography algorithm and to carry out the numerical analysis with no other specific considerations.

For the quantitative evaluation, the normalized mean square error (NMSE) of the estimator is used which is calculated as

$$\text{NMSE} = E \left[ \frac{|h(\mathbf{x}) - \hat{h}(\mathbf{x})|^2}{|h(\mathbf{x})|^2} \right]$$

with  $E[\cdot]$  denoting the expected value.

### 4.2. Numerical Results

**Fig. 1(a)** and **Fig. 1(b)** show the actual generated and estimated maps using  $N = 100$  measurements and  $K = 10$  centroids respectively. As the figures show, the estimated map matches the actual one and can be seen as a smoothed version of it.

Quantitatively, the NMSEs for different values of  $N$  and  $K$  are shown in **Fig. 2**. As expected, the trend is that the larger the number of centroids, the better the performance. Nevertheless, it can also be observed that when the number of centroids approaches the number of measurements, the performance is slightly worse for all the values of  $N$ . This behavior is due to the fact that, when the number of centroids is close to the number of measurements points, the representing centroids locations are closer to the measurements' points and therefore an almost exact interpolation around these points takes place which results in an overfitting and in return an increase of the errors outside these samples.

A comparative study between the proposed non-parametric RBF based cartography and the RKHS-based algorithm proposed in [14] is carried out and the results are shown in **Fig. 3**. For lower values of  $N$  the RKHS based cartography outperforms the non-parametric RBF using 10 centroids with about 2 dB for the used parameters. Notice that [14] assumes the knowledge of transmitters locations and PSDs which compensates having fewer measurements for parametric estimation using RKHS. However, when we increase the number of measurements points, RBF cartography outperforms the RKHS-based algorithm with a cross over when  $N \approx 70$  measurements for our setup. Here the reason is that more measurements enable the RBF method to overcome the lack of transmission parameters knowledge. Moreover, adaptation of the RBF decaying parameters and centroids plays a role here as well.

## 5. CONCLUSIONS

Spatial interpolation for constructing spectrum maps is performed using strategically centered adaptive Gaussian radial basis functions. The centroids locations optimized jointly with the decaying parameters and the weights of the linear model. The findings show the influence of the model order on the proposed algorithm performance.

## 6. REFERENCES

- [1] D. H. Huang, S. H. Wu, W. R. Wu, and P. H. Wang, "Cooperative radio source positioning and power map reconstruction: A sparse bayesian learning approach," *IEEE Trans. Veh. Technol.*, vol. 64, no. 6, pp. 2318–2332, Jun 2015.
- [2] S. Grimoud, S. B. Jemaa, B. Sayrac, and E. Moulines, "A REM enabled soft frequency reuse scheme," in *IEEE Global Commun. Conf.*, Dec 2010, pp. 819–823.
- [3] S. Debroy, S. Bhattacharjee, and M. Chatterjee, "Spectrum map and its application in resource management in cognitive radio networks," *IEEE Trans. Cognitive Commun. and Networking*, vol. 1, no. 4, pp. 406–419, Dec 2015.
- [4] A. Galindo-Serrano, B. Sayrac, S. B. Jemaa, J. Rihijärvi, and P. Mähönen, "Harvesting MDT data: Radio environment maps for coverage analysis in cellular networks," in *8th Int. Conf. Cognitive Radio Oriented Wireless Networks*, Jul 2013, pp. 37–42.
- [5] J. D. Naranjo, A. Ravanshid, I. Viering, R. Halfmann, and G. Bauch, "Interference map estimation using spatial interpolation of MDT reports in cognitive radio networks," in *IEEE Wireless Commun. and Networking Conf.*, Apr 2014, pp. 1496–1501.
- [6] A. B. H. Alaya-Feki, S. B. Jemaa, B. Sayrac, P. Houze, and E. Moulines, "Informed spectrum usage in cognitive radio networks: Interference cartography," in *IEEE 19th Int. Symp. Personal, Indoor and Mobile Radio Commun.*, Sep 2008, pp. 1–5.
- [7] G. Boccolini, G. Hernández-Peñaloza, and B. Beferull-Lozano, "Wireless sensor network for spectrum cartography based on kriging interpolation," in *IEEE 23rd Int. Symp. Personal, Indoor and Mobile Radio Commun.*, Sep 2012, pp. 1565–1570.
- [8] S. J. Kim, E. Dall'Anese, and G. B. Giannakis, "Cooperative spectrum sensing for cognitive radios using kriged kalman filtering," *IEEE J. Sel. Topics Signal Process.*, vol. 5, no. 1, pp. 24–36, Feb 2011.
- [9] S. J. Kim and G. B. Giannakis, "Cognitive radio spectrum prediction using dictionary learning," in *IEEE Global Commun. Conf.*, Dec 2013, pp. 3206–3211.
- [10] J. A. Bazerque and G. B. Giannakis, "Distributed spectrum sensing for cognitive radio networks by exploiting sparsity," *IEEE Trans. Signal Process.*, vol. 58, no. 3, pp. 1847–1862, Mar 2010.
- [11] J. A. Bazerque, G. Mateos, and G. B. Giannakis, "Group-lasso on splines for spectrum cartography," *IEEE Trans. Signal Process.*, vol. 59, no. 10, pp. 4648–4663, Oct 2011.
- [12] G. Ding, J. Wang, Q. Wu, Y. D. Yao, F. Song, and T. A. Tsiftsis, "Cellular-base-station-assisted device-to-device communications in TV white space," *IEEE J. Sel. Areas Commun.*, vol. 34, no. 1, pp. 107–121, Jan 2016.
- [13] D. Romero, S. J. Kim, and G. B. Giannakis, "Online spectrum cartography via quantized measurements," in *49th Ann. Conf. Inform. Sci. and Syst.*, Mar 2015, pp. 1–4.
- [14] D. Romero, S. J. Kim, López-Valcarce, and G. B. Giannakis, "Spectrum cartography using quantized observations," in *IEEE Int. Conf. Acoust., Speech and Signal Process.*, Apr 2015, pp. 3252–3256.
- [15] D. Romero, S. Kim, G. B. Giannakis, and R. López-Valcarce, "Learning power spectrum maps from quantized power measurements," *CoRR*, vol. abs/1606.02679, 2016. [Online]. Available: <http://arxiv.org/abs/1606.02679>
- [16] D. S. Broomhead and D. Lowe, "Radial basis functions, multi-variable functional interpolation and adaptive networks," *Complex Syst.*, vol. 2, pp. 321–355, Mar 1988.
- [17] Y. S. Abu-Mostafa, M. Magdon-Ismael, and H.-T. Lin, *Learning From Data*. AMLBook, 2012.
- [18] R. W. K. Arthur E. Hoerl, "Ridge regression: Applications to nonorthogonal problems," *Technometrics*, vol. 12, no. 1, pp. 69–82, 1970.
- [19] I. S. Dhillon and D. S. Modha, "Concept decompositions for large sparse text data using clustering," *Mach.*, vol. 42, no. 1, pp. 143–175, 2001.
- [20] S. Lloyd, "Least squares quantization in pcm," *IEEE Trans. Inf. Theory*, vol. 28, no. 2, pp. 129–137, Mar 1982.
- [21] W. Yamada, M. Sasaki, T. Sugiyama, O. Holland, S. Ping, B. Yeboah-Akokuwah, J. Hwang, and H. Aghvami, "Indoor propagation model for TV white space," in *9th Int. Conf. Cognitive Radio Oriented Wireless Networks and Commun.*, Jun 2014, pp. 209–214.
- [22] D. H. Kang, K. W. Sung, and J. Zander, "Attainable user throughput by dense WiFi deployment at 5 GHz," in *IEEE 24th Ann. Int. Symp. Personal, Indoor, and Mobile Radio Commun.*, Sep 2013, pp. 3418–3422.